Log-aesthetic curves: Similarity geometry, integrable discretization and variational principles

Inoguchi, Jun-ichi
Department of Mathematics, Hokkaido University

Jikumaru, Yoshiki
Faculty of Information Networking for Innovation and Design, Toyo University

Kajiwara, Kenji
Institute of Mathematics for Industry, Kyushu University

Miura, Kenjiro T.
Graduate School of Science and Technology, Shizuoka University

他

出版情報：Computer Aided Geometric Design. 105, pp.102233-, 2023-09. Elsevier
バージョン：

Computer Aided Geometric Design 105 (2023) 102233

Contents lists available at ScienceDirect

Computer Aided Geometric Design

journal homepage: www.elsevier.com/locate/cagd

Log-aesthetic curves: Similarity geometry, integrable discretization and variational principles ☆

Jun-ichi Inoguchi [a], Yoshiki Jikumaru [b,*], Kenji Kajiwara [c], Kenjiro T. Miura [d], Wolfgang K. Schief [e]

[a] Department of Mathematics, Hokkaido University, Sapporo, 060-0810, Japan
[b] Faculty of Information Networking for Innovation and Design, Toyo University, 1-7-11 Akabanedai, Kita-ku, Tokyo, 115-8650, Japan
[c] Institute of Mathematics for Industry, Kyushu University, 744 Motooka, Fukuoka, 819-0395, Japan
[d] Graduate School of Science and Technology, Shizuoka University, 3-5-1 Johoku, Hamamatsu, 432-8561, Japan
[e] School of Mathematics and Statistics, The University of New South Wales, Sydney 2052, NSW, Australia

ARTICLE INFO

Article history:
Received 5 January 2022
Received in revised form 17 July 2023
Accepted 18 July 2023
Available online 25 July 2023

Keywords:
Log-aesthetic curves
Similarity geometry
Burgers equation
Variational principle
Integrable discretization
Generation of curve

ABSTRACT

In this paper, we consider a class of plane curves called log-aesthetic curves and their generalization which are used in computer aided geometric design. In the framework of similarity geometry, those curves are characterized as invariant curves under the integrable flow on plane curves governed by the Burgers equation. They also admit a variational formulation leading to the stationary Burgers equation as the Euler-Lagrange equation. As an application of the formulation, we propose a discretization of these curves and the associated variational principle which preserves the underlying integrable structure. We finally present algorithms for generating discrete log-aesthetic curves for given G^1 data based on similarity geometry. Our method is able to generate S-shaped discrete curves with an inflection as well as C-shaped curves according to the boundary condition. The resulting discrete curves are regarded as self-adaptive discretization and thus high-quality even with the small number of points. Through the continuous representation, those discrete curves provide a flexible tool for the generation of high-quality shapes.

1. Introduction

1.1. Background and overview

In this paper, we consider a class of plane curves in computer aided geometric design called the *log-aesthetic curve* (LAC) and its generalization called the *quasi aesthetic curve* (qAC). The LAC has been originally proposed by extracting the common properties from thousands of plane curves which car designers regard as aesthetic (Harada et al., 1999). A new

The code (and data) in this article has been certified as Reproducible by Code Ocean: https://codeocean.com/. More information on the Reproducibility Badge Initiative is available at https://www.elsevier.com/physical-sciences-and-engineering/computer-science/journals.

☆ Editor: Konrad Polthier.

* Corresponding author.
E-mail addresses: inoguchi@math.sci.hokudai.ac.jp (J. Inoguchi), jikumaru@toyo.jp (Y. Jikumaru), kaji@imi.kyushu-u.ac.jp (K. Kajiwara), miura.kenjiro@shizuoka.ac.jp (K.T. Miura), w.schief@unsw.edu.au (W.K. Schief).

https://doi.org/10.1016/j.cagd.2023.102233

mathematical characterization of the LAC and the qAC based on the theory of integrable systems and similarity geometry was announced in Inoguchi et al. (2018). In the previous paper (Inoguchi et al., 2018), the LAC and the qAC are formulated as invariant curves with respect to the integrable flow on the plane curves preserving the similarity arc length. More precisely, the evolution of the curves is governed by the similarity curvature which is characterized by the stationary solutions of integrable nonlinear partial differential equation arising from the geometric setting. An alternate formulation based on the variational principle of the LAC and the qAC is presented by introducing the fairing energy functional. We then construct a discrete analogue of the LAC (dLAC) and the qAC (dqAC) within the above-mentioned framework, which gives a new implementation of the LAC and the qAC with a sound mathematical background as discrete curves. In general, discrete curves and surfaces are useful for generating high-quality smooth curves and surfaces without undulations, since it is easier to control the change of curvatures of discrete curves and surfaces than smooth ones (see, for example, Kobayashi and Kimura (2010)). Practically, it is easier to deform the dLAC than the LAC since a dLAC is a set of discrete points, which is suitable for flexible design process in CAD. For manufacturing process, continuous representation of the dLAC is crucial, but approximating a dLAC by NURBS curves gives us a high-quality shape, since the curvature distribution is well preserved through this approximation. Therefore the dLAC serves as a fundamental ingredient for flexible and high-quality shape generation by the LAC. Then the contributions of this paper may be described as follows:

(1) The technique of integrable discretization is applied to define the dLAC and the dqAC, together with the formulation by the discrete variational principle. We then introduce a discrete fairing functional and formulate these discrete curves in terms of a discrete variational principle. The discrete curves obtained in this manner are not naïve approximations of the original LAC and qAC but admit their own natural geometric characterization.
(2) An implementation of the dLAC is presented, in which we consider the boundary value problem of the dLAC for given endpoints and associated tangent vectors. In this implementation, the dLAC serves as a self-adaptive mesh discretization of the LAC. In general, discrete curves have more degrees of freedom in design than smooth curves due to the parameters which disappear in the continuum limit, so that generation of various shapes is possible. The dLAC proposed in this paper consists of mathematically defined discrete points on a certain curve, which is expected to be useful for various designs, as it can generate wide variety of shapes.
(3) The continuous representation of discrete curves is indispensable for application of discrete curves to various manufacturing in order to guarantee the precision of the products to be made. The discrete points of a dLAC are defined mathematically and are without unnecessary noise, which is different from the measurement data of the reverse engineering. The B-spline or the NURBS curves can approximate the shape generated by the dLAC precisely including the curvature distribution. Therefore the dLAC can be directly applicable to manufacturing and provides with a flexible tool for high-quality shape generation.

1.2. Related works

The class of qAC was introduced in Sato and Shimizu (2016), see also Inoguchi (2016); Inoguchi et al. (2018). Another generalization of the LAC (GLAC) introduced in Gobithaasan and Miura (2011) is also well studied, and the GLAC is characterized by the linearity of the logarithmic curvature/torsion graphs (Gobithaasan et al., 2014b), Bernoulli equations (Miura et al., 2015), and similarity geometric context (Inoguchi et al., 2019). Some attempts of variational characterizations of "log-aesthetic surfaces" are studied in Suzuki et al. (2018a,b). Applications of the LAC are, for instance, shape completion problems (Gobithaasan et al., 2014d), log-aesthetic magnetic curves to CAD systems (Wo et al., 2014), approximation of the LAC/GLAC using quintic Bézier curves for industrial CAD systems (Albayari et al., 2017; Lu and Xiang, 2016). On the generation of the LAC, representative studies are the adaptive Runge-Kutta methods (Gobithaasan et al., 2014c), evolution of a curve by log-aesthetic flow (Miura et al., 2017) for solving the equation, generation of a LAC segment for a given G^2 Hermite data (Gobithaasan et al., 2014a; Wo et al., 2015), and an explicit formula of the smooth LAC in terms of the incomplete Gamma function (Ziatdinov et al., 2012). In the previous studies, generating methods of the S-shaped LAC are based on connecting two independent C-shaped LACs at some "inflection point" as in Gobithaasan et al. (2014a,d); Miura et al. (2013), however, we propose an essentially different method of the generation of the S-shaped dLAC. Similarity geometric approaches to the LAC/GLAC are also studied in Inoguchi et al. (2019); Miura et al. (2018).

2. Log-aesthetic curves and similarity geometry

In this section, we give a brief review of the LAC and the qAC based on similarity geometry according to Inoguchi et al. (2018). Originally, the LAC has been studied in the framework of Euclidean geometry. Before proceeding to the LAC, we give a brief account of the treatment of plane curves in Euclidean geometry. Let $\gamma(s) \in \mathbb{R}^2$ be an arc length parametrized plane curve and s be arc length. We introduce the Frenet frame by $F^{\mathrm{E}}(s) = (T^{\mathrm{E}}(s), N^{\mathrm{E}}(s)) \in \mathrm{SO}(2)$, where $d\gamma(s)/ds = T^{\mathrm{E}}(s)$ and $N^{\mathrm{E}}(s) = JT^{\mathrm{E}}(s)$ are the tangent and the normal vector fields, respectively, and J is the positive $\pi/2$-rotation. The Frenet frame satisfies the *Frenet formula*

$$\frac{dF^{\mathrm{E}}(s)}{ds} = F^{\mathrm{E}}(s)L^{\mathrm{E}}(s), \quad L^{\mathrm{E}}(s) = \begin{pmatrix} 0 & -\kappa(s) \\ \kappa(s) & 0 \end{pmatrix}, \tag{1}$$

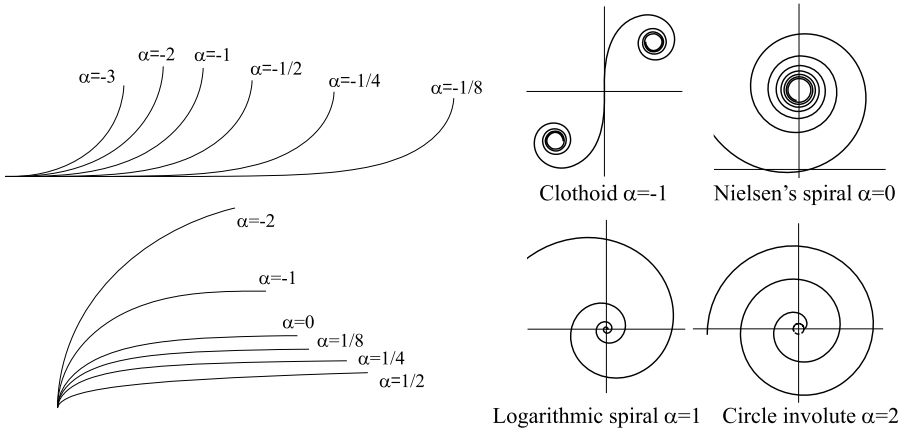

Fig. 1. Left: Log-aesthetic curves for various parameters. Right: Log-aesthetic curves for $\alpha = -1, 0, 1, 2$.

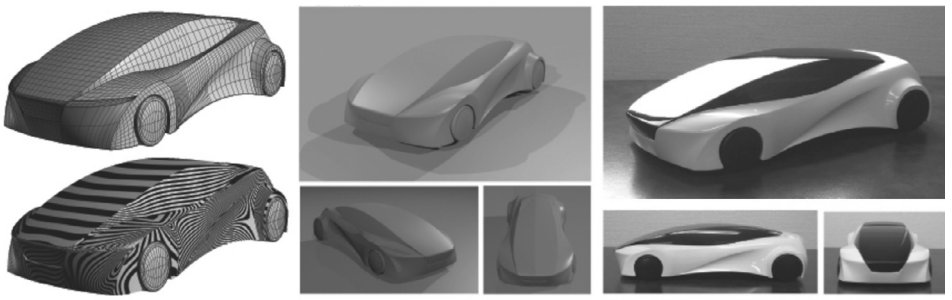

(a) Iso-lines and zebra mapping (b) Rendering (c) Mock-up

Fig. 2. A car model designed by means of log-aesthetic (LA) splines and its mock-up (Miura et al., 2013).

where $\kappa(s)$ is the curvature. Since $|T^{\mathrm{E}}(s)| = 1$ by definition of arc length, we may write $T^{\mathrm{E}}(s) = {}^t(\cos\theta(s), \sin\theta(s))$, where θ is called the *angle function*. Note that the curvature κ is related to the signed radius of curvature $q(s)$ and the angle function $\theta(s)$ by $q(s) = 1/\kappa(s)$, $\kappa(s) = d\theta(s)/ds$.

According to Miura (2006), an arc length parametrized plane curve $\gamma(s) \in \mathbb{R}^2$ is said to be a LAC of slope α if its signed curvature radius q satisfies

$$q(s)^\alpha = as + b \quad (\alpha \neq 0), \quad q(s) = \exp(as + b) \quad (\alpha = 0), \quad a, b \in \mathbb{R}. \tag{2}$$

The class of LAC includes some well known plane curves. For instance, the logarithmic spiral, the clothoid, the Nielsen spiral are included as the LAC of slope 1, -1, and 0, respectively. The LAC of slope 2 is also known as the circle involute curve. These examples are illustrated in Fig. 1.

LACs are now maturing in industrial and graphic design practices. Fig. 2 shows the practical example of a car designed using the LA splines. Fig. 2(a) shows free-form surface iso-parametric lines generated using the LA splines and corresponding zebra maps. Fig. 2(b) shows the geometric model with a special lighting condition and 2(c) are photos of a manufactured mockup based on the geometric model. Note that the roof of the car is designed by an LA spline curve with three segments and its zebra maps indicate that the surface is of high quality. Based on our experience, the LA splines are generated with most G^2 Hermite data. Another direction of application is developed in architecture design (Suzuki, 2017). For more details of the LAC, we refer to Inoguchi et al. (2019); Miura and Gobithaasan (2014, 2016).

Those studies have been carried out based on the basic characterization (2) in the framework of Euclidean geometry. However, equation (2) is too simple to identify the underlying geometric structure. Consequently, we do not have a good guideline as to how to generate a larger class of aesthetic geometric objects including the LAC based on a sound mathematical background. As we have announced in the previous paper (Inoguchi et al., 2018), it is natural to adopt the framework of similarity geometry, which is a Klein plane geometry associated with the group of similarity transformations, *i.e.*, isometries and scalings. The natural parameter of plane curves in similarity geometry is the angle function $\theta = \int \kappa(s)\, ds$, which will be referred to as the *similarity arc length* in this paper. For simplicity, we assume that the curves have no inflection points. Let $\gamma(\theta) \in \mathbb{R}^2$ be a plane curve in similarity geometry parametrized by the similarity arc length θ. We introduce the similarity Frenet frame $F(\theta)$ by

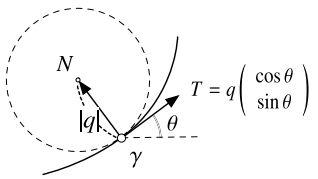

Fig. 3. Description of plane curves in similarity geometry.

$$F(\theta) = (T, N) \in \mathrm{CO}^+(2) = \{rA \,|\, r \in \mathbb{R}_+,\ A \in \mathrm{SO}(2)\}, \quad T = \frac{d\gamma}{d\theta}, \quad N = J\frac{d\gamma}{d\theta}, \tag{3}$$

where T and N are the similarity tangent and normal vector fields, respectively. The group $\mathrm{CO}^+(2)$ is called the *conformal orthogonal group*. Note that $|T(\theta)| = |q|$ which follows from $|T^{\mathrm{E}}(s)| = 1$ and $d\theta/ds = \kappa = 1/q$ (see Fig. 3). Then, the (Euclidean) Frenet formula (1) implies that the similarity Frenet frame satisfies the *similarity Frenet formula*

$$\frac{dF}{d\theta} = FL, \quad L = \begin{pmatrix} -u & -1 \\ 1 & -u \end{pmatrix}, \tag{4}$$

for some function $u(\theta)$ which is called the *similarity curvature*. Moreover, the similarity curvature u is related to the signed curvature radius q by the *Cole-Hopf transformation*:

$$u = -\frac{1}{q}\frac{dq}{d\theta}. \tag{5}$$

One can check that a plane curve without inflection points in similarity geometry is uniquely determined by the similarity curvature up to similarity transformations.

Remark 2.1. The similarity arc length parameter θ is defined only if the curve has no inflection points. Therefore, only curves with isolated inflection points possess a piecewise natural parameter θ.

The notion of the LAC may be shown to be invariant under the similarity transformations. For instance, the slope α is expressed as $\alpha = 1 + (1/u^2)\,du/d\theta$. In other words, the LAC is reformulated in terms of similarity geometry as follows (Inoguchi, 2016; Sato and Shimizu, 2015). A plane curve $\gamma(\theta)$ in similarity geometry is said to be a qAC of slope α if its similarity curvature satisfies the Riccati equation (Sato and Shimizu, 2016)

$$\frac{du}{d\theta} = (\alpha - 1)u^2 + c, \quad c \in \mathbb{R}. \tag{6}$$

In particular, if $c = 0$, then γ is said to be a LAC of slope α, where the equation for the similarity curvature and its solution are explicitly given by

$$\frac{du}{d\theta} = (\alpha - 1)u^2, \tag{7}$$

$$u = -\frac{\lambda}{(\alpha - 1)\lambda\theta + 1}, \quad \lambda \in \mathbb{R}, \tag{8}$$

respectively. Under the framework of similarity geometry, it is known that there are two characterizations of the LAC and the qAC. One of the characterizations is given by considering the integrable (time) evolution of plane curves that preserves the invariant parameter of similarity geometry, which is known to be described by the Burgers hierarchy (Chou and Qu, 2002). The simplest evolution is given by

$$\frac{\partial}{\partial t}\gamma = (b - u)T - N, \quad b \in \mathbb{R}, \tag{9}$$

$$\frac{\partial F}{\partial t} = FM, \quad M = \begin{pmatrix} -\frac{\partial u}{\partial \theta} + u^2 + 1 - bu & -b \\ b & -\frac{\partial u}{\partial \theta} + u^2 + 1 - bu \end{pmatrix}, \tag{10}$$

in terms of the position vector γ and the similarity Frenet frame F, respectively. The compatibility condition of (4) and (10) $(F_t)_\theta = (F_\theta)_t$, or equivalently $\partial L/\partial t - \partial M/\partial\theta = LM - ML$ yields the *Burgers equation*

$$\frac{\partial u}{\partial t} = \frac{\partial}{\partial \theta}\left(\frac{\partial u}{\partial \theta} - u^2 + bu\right). \tag{11}$$

Therefore, the evolution is referred to as the *Burgers flow*. The Burgers equation is linearized in terms of the signed curvature radius via the Cole-Hopf transformation (5) according to

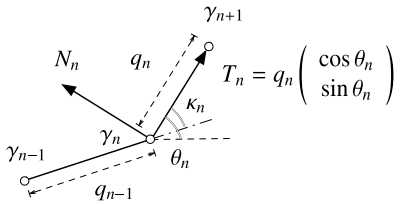

Fig. 4. Description of discrete plane curves in similarity geometry.

$$\frac{\partial q}{\partial t} = \frac{\partial^2 q}{\partial \theta^2} + b\frac{\partial q}{\partial \theta}.$$

Imposing the *stationarity ansatz* $\partial u/\partial t = 0$ reduces the Burgers equation (11) to the Riccati equation

$$\frac{\partial u}{\partial \theta} = u^2 - bu + c, \quad c \in \mathbb{R}. \tag{12}$$

In particular, putting $b = 0$, we recover the Riccati equation (6) with $\alpha = 2$. We note that (6) is obtained formally from (12) by making the substitution $u \to (\alpha - 1)u$. In this sense, qACs are characterized by the stationary Burgers flow, or in other words, they are invariant curves with respect to the Burgers flow. We also note that the parameter b corresponds to a rotation of the curve.

Another characterization of the LAC and the qAC is the variational formulation with respect to the *fairing energy functional* $\mathcal{F}^{\lambda,a}$ (Inoguchi et al., 2018).

$$\mathcal{F}^{\lambda,a}(\gamma) = \int_{\theta_1}^{\theta_2} \frac{1}{2}\left\{a^2 u(\theta)^2 + \lambda\left(\frac{q_1 q_2}{q(\theta)^2}\right)^a\right\} d\theta, \tag{13}$$

where $a = \alpha - 1$, λ is an arbitrary constant and $q_i = q(\theta_i)$ $(i = 1, 2)$. In fact, we have:

Theorem 2.2 *(Inoguchi et al. (2018)). If a plane curve γ is a critical point of the fairing energy $\mathcal{F}^{\lambda,a}$ (13) under the assumption of preservation of the total turning angle and the boundary condition that the ratio of the length of tangent vectors at the endpoints is preserved, then the similarity curvature u satisfies $u' = au^2 + c$, where c is a constant. Therefore, quasi aesthetic curves of slope $\alpha \neq 1$ are critical points of the fairing functional.*

In summary, the LAC and the qAC have two characterizations under the framework of similarity geometry; one characterization is as the invariant curves of the integrable time evolution of plane curves, and the other is as a critical point of the fairing energy functional. In the following sections, we consider a natural discretization of the LAC and the qAC based on these characterizations.

3. Discrete log-aesthetic curves and quasi aesthetic curves

One of the benefits of the formulation presented in Section 2 is that one is led to the construction of a natural discrete analogue of the LAC and the qAC which preserves the underlying integrable nature of these curves. It is expected that these discrete curves obtained on the principle of structure preservation have better quality as discrete curves compared to other existing discretizations regarded as approximations (cf. Section 5). In this section, we construct the discrete analogue of the LAC and the qAC by using the framework of integrable evolution of discrete plane curves in similarity geometry as discussed in Kajiwara et al. (2016). Let $\gamma_n \in \mathbb{R}^2$, $n \in \mathbb{Z}$ be a discrete plane curve. As shown in Fig. 4, we introduce the *similarity Frenet frame* $F_n \in \mathrm{CO}^+(2)$ according to

$$F_n = (T_n, N_n), \quad T_n = \gamma_{n+1} - \gamma_n, \quad N_n = JT_n, \tag{14}$$

where T_n and N_n are discrete tangent and normal vectors, respectively, and we write

$$q_n = |T_n| = \sqrt{\langle T_n, T_n\rangle}. \tag{15}$$

Then, F_n satisfies the *discrete similarity Frenet formula*

$$\begin{aligned} &F_{n+1} = F_n L_n, \quad L_n = u_n R(\kappa_{n+1}), \quad R(\kappa_{n+1}) = \begin{pmatrix} \cos\kappa_{n+1} & -\sin\kappa_{n+1} \\ \sin\kappa_{n+1} & \cos\kappa_{n+1} \end{pmatrix}, \\ &u_n = \frac{q_{n+1}}{q_n}, \quad \kappa_n = \angle(T_{n-1}, T_n). \end{aligned} \tag{16}$$

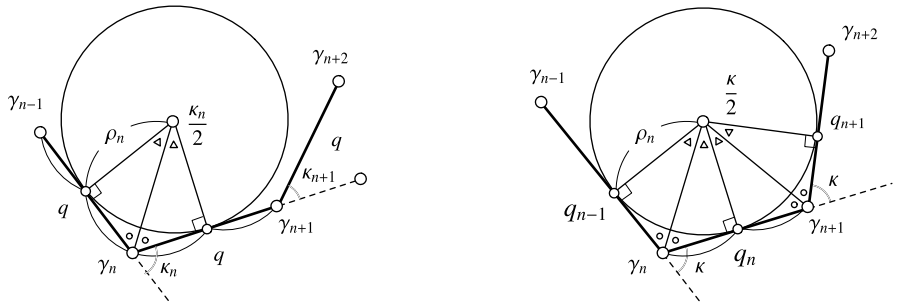

Fig. 5. Radii of osculating circles of an arc length parametrized discrete plane curve in Euclidean geometry and a discrete curve of constant turning angle in similarity geometry. Left: Euclidean geometry, $|\gamma_{n+1}-\gamma_n| = q_n = \text{const}$. Right: similarity geometry, $\angle(\gamma_n-\gamma_{n-1}, \gamma_{n+1}-\gamma_n) = \kappa_n = \text{const}$. In both cases, the radii are given by $\rho_n = (q_n/2)\cot(\kappa_n/2)$.

Hereafter, we assume that the discrete turning angle $\kappa_n = \kappa = \text{const}$.. The associated discrete curves may be regarded as the similarity geometric analogues of arclength parametrized discrete curves in Euclidean geometry. Such discrete curves may be referred to as "*similarity arc length parametrized*". In this case, u_n plays the role of a discrete counterpart of the similarity curvature of smooth plane curves.

Remark 3.1. There is an interesting correspondence on the radii of osculating circles for both arc length parametrized discrete curves in Euclidean geometry and similarity geometry (see Fig. 5). In Euclidean geometry, a discrete plane curve $\gamma_n \in \mathbb{R}^2$ is said to be an arc length parametrized discrete curve if the segment length is a constant (Hoffmann, 2009), i.e., $|\gamma_{n+1}-\gamma_n| = q = \text{const}$. Then, there exists a circle touching the two segments $\gamma_n - \gamma_{n-1}$ and $\gamma_{n+1}-\gamma_n$ at their midpoints, and its radius ρ_n is given by $\rho_n = (q/2)\cot(\kappa_n/2)$, where $\kappa_n = \angle(\gamma_n-\gamma_{n-1}, \gamma_{n+1}-\gamma_n)$. On the other hand, in similarity geometry, there exists a circle touching simultaneously the three consecutive segments $\gamma_n-\gamma_{n-1}$, $\gamma_{n+1}-\gamma_n$, $\gamma_{n+2}-\gamma_{n+1}$ with the second segment being touched at its midpoint. The radius of the circle ρ_n is given by $\rho_n = (q_n/2)\cot(\kappa/2)$, which is the same expression as in the Euclidean case. From this observation one may regard $1/\rho_n$ as a discrete analogue of the Euclidean curvature, and one can trace its change along the discrete curve by $1/q_n$.

We consider an integrable discrete (time) evolution of a discrete curve γ_n preserving the constant turning angle $\kappa_n = \kappa$. We denote the original discrete curve by γ_n^0 and the curve obtained after m discrete time steps is labelled by γ_n^m. The quantities relevant to these discrete curves are written in a similar manner. For example, $q_n^m = |\gamma_{n+1}^m - \gamma_n^m|$ and $u_n^m = q_{n+1}^m/q_n^m$. Then, the simplest evolution is known to be given by Kajiwara et al. (2016)

$$\gamma_n^{m+1} = \gamma_n^m - \frac{\sigma}{\kappa^2}\left\{\left(\frac{1}{u_{n-1}^m} - \cos\kappa\right)T_n^m + \sin\kappa\, N_n^m\right\}, \tag{17}$$

where the frame F_n^m satisfies

$$\begin{aligned} &F_{n+1}^m = F_n^m L_n^m, \quad L_n^m = u_n^m R(\kappa), \\ &F_n^{m+1} = F_n^m M_n^m, \quad M_n^m = H_n^m I, \quad I: \text{identity matrix}, \quad H_n^m = 1 + \frac{\sigma}{\kappa^2}\left(u_n^m - 2\cos\kappa + \frac{1}{u_{n-1}^m}\right), \end{aligned} \tag{18}$$

and σ is a constant. Note that the first equation is nothing but the discrete similarity Frenet formula. The compatibility condition of (18), $(F_{n+1})^{m+1} = (F^{m+1})_{n+1}$, or equivalently, $L_n^{m+1}M_n^m = M_{n+1}^m L_n^m$, yields the *discrete Burgers equation* (Hirota, 1979; Nishinari and Takahashi, 1998)

$$\frac{u_n^{m+1}}{u_n^m} = \frac{1+\frac{\sigma}{\kappa^2}\left(u_{n+1}^m - 2\cos\kappa + \frac{1}{u_n^m}\right)}{1+\frac{\sigma}{\kappa^2}\left(u_n^m - 2\cos\kappa + \frac{1}{u_{n-1}^m}\right)}, \tag{19}$$

which is an integrable discretization of the Burgers equation (11) in a sense that it preserves the linearizability. Actually, (19) is linearized in terms of q_n^m to

$$\frac{q_n^{m+1}-q_n^m}{\sigma} = \frac{q_{n+1}^m - 2\cos\kappa\, q_n^m + q_{n-1}^m}{\kappa^2}. \tag{20}$$

Note that the continuum limit (11) of (19) with $b=0$ is obtained by setting

$$u_n^m = 1 - \kappa u(t,\theta), \quad \theta = n\kappa, \quad t = m\sigma, \tag{21}$$

and taking the limit $\kappa, \sigma \to 0$. In fact, substituting (21) into (19) and expanding in terms of κ and σ by noticing

$$u_{n\pm1}^m = 1 - \kappa u(t, \theta \pm \kappa) = 1 - \kappa\left(u \pm \kappa \frac{\partial u}{\partial \theta} + \frac{\kappa^2}{2}\frac{\partial^2 u}{\partial \theta^2} + \cdots\right), \quad u_n^{m+1} = 1 - \kappa u(t+\sigma, \theta) = 1 - \kappa\left(u + \sigma \frac{\partial u}{\partial t} + \cdots\right), \tag{22}$$

we see that the discrete Burgers equation (19) becomes

$$\frac{\partial u}{\partial t} = \frac{\partial^2 u}{\partial \theta^2} - 2u\frac{\partial u}{\partial \theta}, \tag{23}$$

which is the Burgers equation (11) with $b = 0$.

Imposing the stationarity ansatz $u_n^{m+1} = u_n^m$ on the discrete Burgers equation (19) and neglecting the superscript m, we obtain the discrete stationary Burgers equation

$$u_{n+1} + \frac{1}{u_n} = u_n + \frac{1}{u_{n-1}}, \tag{24}$$

whose continuum limit according to (21) gives the stationary Burgers equation

$$\frac{d^2 u}{d\theta^2} = 2u\frac{du}{d\theta}. \tag{25}$$

Equation (24) can be integrated to yield the discrete Riccati equation

$$u_{n+1} + \frac{1}{u_n} = C, \tag{26}$$

where C is an integration constant. The existence of the continuum limit of (26) according to (21) requires the parametrization $C = 2 - c\kappa^2$, leading to

$$\frac{du}{d\theta} = u^2 + c. \tag{27}$$

In order to construct the discrete analogue of (7) and (6), we replace u_n by $(u_n)^a$, where $a = \alpha - 1$, to obtain

$$(u_{n+1})^a + \frac{1}{(u_n)^a} = (u_n)^a + \frac{1}{(u_{n-1})^a}, \tag{28}$$

and

$$(u_{n+1})^a + \frac{1}{(u_n)^a} = C, \tag{29}$$

respectively. This a dependence is motivated by the following observation. In the smooth curve case, the similarity curvature $u = -(\log q)_\theta$ is replaced by au, which implies that the curvature radius q is replaced by q^a. In the discrete case, as explained in Remark 3.1 and Fig. 5, we have $u_n = q_{n+1}/q_n = \rho_{n+1}/\rho_n$, where $\rho_n = (q_n/2)\cot(\kappa/2)$ is the radius of an analogue of the curvature circle, which implies the above a dependence on u_n. Indeed, this a dependence is consistent with the parametrization (21). Actually, noticing that $(u_n)^a = (1 - \kappa u)^a = 1 - au\kappa + O(\kappa^2)$, we see that (28) and (29) reduce to (7) and (6), respectively, if we set $C = 2 - ac\kappa^2$. Let us consider the solution of (29), which may be linearized in terms of $(q_n)^a$ as

$$\frac{(q_{n+1})^a - 2(q_n)^a + (q_{n-1})^a}{\kappa^2} = -ac(q_n)^a, \tag{30}$$

by noticing

$$(u_n)^a = \frac{(q_{n+1})^a}{(q_n)^a}. \tag{31}$$

In the case $c = 0$, the solution of (30) is given by $(q_n)^a = c_1 n + c_2$ with c_1, c_2 being arbitrary constants to yield

$$u_n = \left(1 + \frac{a\lambda\kappa}{a\lambda\kappa n + 1}\right)^{\frac{1}{a}}, \tag{32}$$

where $\lambda = c_1/(\kappa a c_2)$. It is evident that under the parametrization (21), (32) yields the original expression for the similarity curvature of the LAC (8), which can be verified by expanding $u_n = (1 + a\lambda\kappa/(a\lambda\theta + 1))^{1/a}$ by κ and comparing with the first equation of (21). The above discussion motivates the following natural definition.

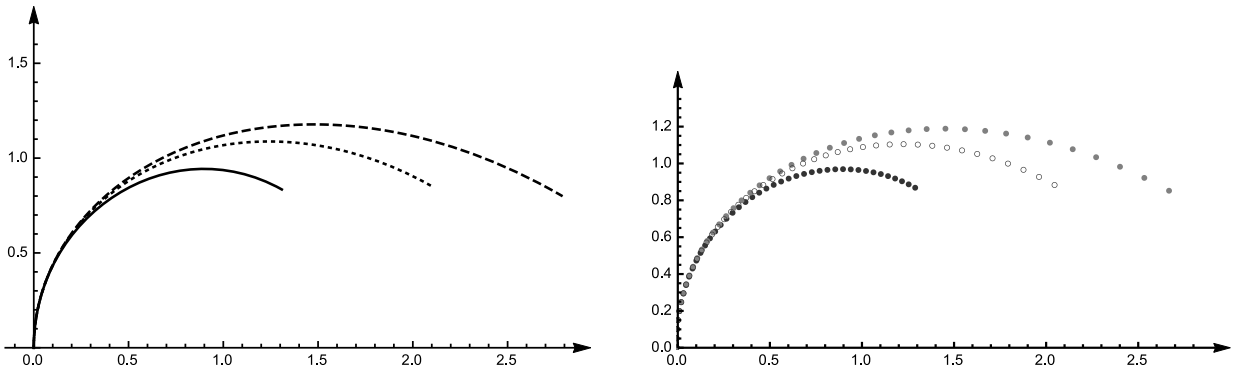

Fig. 6. Smooth and discrete quasi aesthetic curves. Left: Quasi aesthetic curves with (i) $(a, c) = (1, 0)$ (solid line), (ii) $(3/2, -1)$ (dashed line), (iii)$(3, -2/3)$ (dotted line). Right: Discrete quasi aesthetic curves with the same parameters (i): black, (ii): gray (iii): white, where $C = 2 - ac\kappa^2$ and $\kappa = 0.05$.

Definition 3.2. Let γ_n be a discrete plane curve of constant turning angle κ. γ_n is said to be a discrete log-aesthetic curve (dLAC) of slope α if u_n satisfies

$$(u_{n+1})^a + \frac{1}{(u_n)^a} = 2. \tag{33}$$

γ_n is said to be a discrete quasi aesthetic curve (dqAC) of slope α if u_n satisfies

$$(u_{n+1})^a + \frac{1}{(u_n)^a} = C, \quad C \in \mathbb{R}. \tag{34}$$

In both cases, $a = \alpha - 1$, and the segment length q_n satisfies

$$(q_{n+1})^a - C(q_n)^a + (q_{n-1})^a = 0. \tag{35}$$

Fig. 6 illustrates some qACs and dqACs with the same parameters a and c.

4. Variational formulation of discrete log-aesthetic curves and discrete quasi aesthetic curves

It turns out that, as in the continuous case, the dLAC and the dqAC proposed in Section 3 may be obtained via a variational principle. Indeed, in the following, we demonstrate that the dLAC and the dqAC may be characterized as the stationary curves of constant turning angle of the *discrete fairing energy functional* $\Phi^{\lambda,a}$ given by

$$\Phi^{\lambda,a}(\gamma) = \sum_{n=n_1}^{n_2-1} \left\{ (u_n)^a + \frac{1}{(u_n)^a} + \lambda \left(\frac{q_{n_1} q_{n_2}}{q_n q_{n+1}} \right)^a \right\}, \tag{36}$$

with respect to an arbitrary variation of the discrete curve γ_n which we write as

$$\delta\gamma_n = \xi_n T_n + \eta_n N_n. \tag{37}$$

To this end, we first compute the variation of the frame by using the discrete similarity Frenet formula (16) as

$$\delta T_n = \delta\gamma_{n+1} - \delta\gamma_n = \chi_n T_n + \psi_n N_n, \quad \delta N_n = -\psi_n T_n + \chi_n N_n, \tag{38}$$

or

$$\delta F_n = F_n M_n, \quad M_n = \begin{pmatrix} \chi_n & \psi_n \\ -\psi_n & \chi_n \end{pmatrix}, \tag{39}$$

where

$$\begin{aligned} \chi_n &= \xi_{n+1} u_n \cos\kappa_{n+1} - \eta_{n+1} u_n \sin\kappa_{n+1} - \xi_n, \\ \psi_n &= \xi_{n+1} u_n \sin\kappa_{n+1} + \eta_{n+1} u_n \cos\kappa_{n+1} - \eta_n. \end{aligned} \tag{40}$$

The variation of the frame (39) must be compatible with the similarity Frenet formula (16). Accordingly, the associated compatibility condition $(\delta F)_{n+1} = \delta(F_{n+1})$, or equivalently, $\delta L_n = L_n M_{n+1} - M_n L_n$ results in the pair

$$\begin{aligned}
\frac{\delta u_n}{u_n}\cos\kappa_{n+1} - \delta\kappa_{n+1}\sin\kappa_{n+1} &= \cos\kappa_{n+1}(\chi_{n+1}-\chi_n) + \sin\kappa_{n+1}(\psi_{n+1}-\psi_n),\\
\frac{\delta u_n}{u_n}\sin\kappa_{n+1} + \delta\kappa_{n+1}\cos\kappa_{n+1} &= -\cos\kappa_{n+1}(\psi_{n+1}-\psi_n) + \sin\kappa_{n+1}(\chi_{n+1}-\chi_n),
\end{aligned} \tag{41}$$

from which we obtain the variation of u_n and κ_n as

$$\frac{\delta u_n}{u_n} = \chi_{n+1}-\chi_n, \quad \delta\kappa_{n+1} = \psi_n - \psi_{n+1}. \tag{42}$$

Taking the variation of $q_n^2 = \langle T_n, T_n\rangle$, we have $2q_n\delta q_n = 2\langle \delta T_n, T_n\rangle$. Then, from (39), we obtain the variation of q_n as

$$\frac{\delta q_n}{q_n} = \chi_n. \tag{43}$$

Note that δu_n can also be calculated by using $u_n = q_{n+1}/q_n$, which is consistent with (42).

On use of the variations (42) and (43), the variation of the discrete fairing energy functional is seen to be

$$\begin{aligned}
\delta\Phi^{\lambda,a}(\gamma) &= a\sum_{n=n_1}^{n_2-1}\left[\left\{(u_n)^a - \frac{1}{(u_n)^a}\right\}\frac{\delta u_n}{u_n} + \lambda\left(-\frac{\delta q_n}{q_n} - \frac{\delta q_{n+1}}{q_{n+1}} + \frac{\delta q_{n_1}}{q_{n_1}} + \frac{\delta q_{n_2}}{q_{n_2}}\right)\left(\frac{q_{n_1}q_{n_2}}{q_nq_{n+1}}\right)^a\right]\\
&= a\sum_{n=n_1}^{n_2-1}\left[\left\{(u_n)^a - \frac{1}{(u_n)^a}\right\}(\widetilde{\chi}_{n+1}-\widetilde{\chi}_n) - \lambda\left(\frac{q_{n_1}q_{n_2}}{q_nq_{n+1}}\right)^a(\widetilde{\chi}_{n+1}+\widetilde{\chi}_n)\right]\\
&= -a\sum_{n=n_1+1}^{n_2-2}\left\{1+\frac{1}{(u_{n-1}u_n)^a}\right\}\left\{(u_n)^a - (u_{n-1})^a + \lambda\left(\frac{q_{n_1}q_{n_2}}{q_{n-1}q_n}\right)^a\right\}\widetilde{\chi}_n\\
&\quad + a\left[(u_{n_2-1})^a - \frac{1}{(u_{n_2-1})^a} + (u_{n_1})^a - \frac{1}{(u_{n_1})^a} - \lambda\left(\frac{q_{n_1}}{q_{n_2-1}}\right)^a + \lambda\left(\frac{q_{n_2}}{q_{n_1+1}}\right)^a\right]\frac{\chi_{n_2}-\chi_{n_1}}{2},
\end{aligned} \tag{44}$$

where

$$\widetilde{\chi}_n = \chi_n - \frac{\chi_{n_1}+\chi_{n_2}}{2}. \tag{45}$$

The boundary term vanishes iff $\chi_{n_1} = \chi_{n_2}$, which implies that $\delta(q_{n_1}/q_{n_2}) = 0$ from (43). This means that the ratio of the length of segments at the endpoints is preserved by the variation, which is the discrete analogue of the boundary condition in the smooth curve case. The first variation formula (44) implies that if γ_n is a critical point of the discrete fairing energy for variations which respect the boundary condition $\delta(q_{n_1}/q_{n_2}) = 0$, then γ_n satisfies

$$(u_n)^a - (u_{n-1})^a + \lambda\left(\frac{q_{n_1}q_{n_2}}{q_{n-1}q_n}\right)^a = 0, \quad n = n_1+1,\dots,n_2-1, \tag{46}$$

which is equivalent to (28) or (26) together with $u_n = q_{n+1}/q_n$ in the same manner as in the continuous case. As a result, we have the following theorem.

Theorem 4.1. *If a discrete plane curve γ_n is a critical point of the discrete fairing energy $\Phi^{\lambda,a}$ (36) under the boundary condition that the ratio of length of segments at the endpoints is preserved, then u_n satisfies (24). Therefore, discrete quasi aesthetic curves of slope $\alpha \neq 1$ are those discrete curves of constant turning angle which constitute critical points of the discrete fairing functional.*

Remark 4.2. Since ψ_n does not enter the variation (44) of the discrete fairing functional, whether or not the variation of the curve preserves the constancy of the turning angle does not affect the discrete Euler-Lagrange equation. However, if $\kappa_{n+1} = \kappa_n$ is to be preserved by the variation then, by virtue of (42), ψ_n is no longer arbitrary but constrained by $\psi_{n+1} - \psi_n = \text{const}$. It is also observed that the structure of the variation (44) may be interpreted in a simple geometric manner. Since, up to Euclidean motions, a discrete curve is uniquely determined by the angles κ_n and the lengths q_n of the segments, we may regard δq_n as independent quantities in the variation of the energy functional. More precisely, in order to respect invariance under similarity transformations, appropriate independent variations are given by $\delta\tilde{q}_n$, where $\tilde{q}_n = q_n/\sqrt{q_{n_1}q_{n_2}}$. Hence, since the energy functional depends on $\tilde{q}_n$ only with $u_n = \tilde{q}_{n+1}/\tilde{q}_n$, its variation may be expressed entirely in terms of $\widetilde{\phi}_n = \delta\tilde{q}_n/\tilde{q}_n$. In this manner, one retrieves the variation (44) if one takes into account that, for instance, $q_{n_1}/q_{n_2-1} = 1/\tilde{q}_{n_2-1}\tilde{q}_{n_2}$.

5. Generation of discrete log-aesthetic curves

In this section, we consider the problem of G^1 Hermite interpolation by using the dLAC, namely, we generate the dLAC with specified endpoints and the direction of segments (tangent vectors) at the endpoints. This problem was formulated and solved for the LAC in Yoshida and Saito (2006). In Section 5.1 we present a method to generate the dLAC based on similarity geometry. In this formulation, we assume that the discrete curves are similarity arc length parametrized; it has a constant turning angle, or, each angle between the adjacent segments is the same, and the segment length q_n is the variables. This implies that this method can generate dLACs without inflection, namely "C-shaped" curves only. On the other hand, the curve segments with an inflection point, namely "S-shaped" curves are also important in industrial design (Miura et al., 2013). A method of generating a LAC with an inflection point has been proposed in Miura et al. (2013) when the slope α is negative. In Section 5.2, we present a method to generate an S-shaped dLAC based on similarity geometry. Also, we construct continuous models from the generated dLACs, and show that the points and the curvatures are well approximated. Thus, dLACs can be directly used for manufacturing.

5.1. Discrete log-aesthetic curves without inflection

We consider a generation method of the dLAC without inflection based on similarity geometry. As mentioned above, we assume that the discrete curve is similarity arc length parametrized. For simplicity, we first construct the dLAC consisting of four points for given endpoints, γ_0 and γ_3, and the direction of the segments at those points with the specified parameter a. Consider the triangle on the plane shown in Fig. 7. The problem is equivalent to determining γ_1 on AB and γ_2 on BC such that $\angle(\gamma_2-\gamma_1, \mathrm{AB}) = \angle(\mathrm{BC}, \gamma_3-\gamma_2) = \kappa$, where $\kappa = \frac{1}{2}\theta_2$. In other words, the length of the segments $q_n = |\gamma_{n+1}-\gamma_n|$ $(n=0,1,2)$ is subject to the constraints

$$q_0\cos\theta_1 + q_1\cos(\theta_1-\kappa) + q_2\cos(\theta_1-2\kappa) = \ell, \tag{47}$$

$$q_0\sin\theta_1 + q_1\sin(\theta_1-\kappa) + q_2\sin(\theta_1-2\kappa) = 0, \tag{48}$$

where we have chosen the coordinates such that $\gamma_0 = {}^t(0,0)$ and $\gamma_3 = {}^t(\ell,0)$ $(\ell>0)$ without loss of generality. Moreover, according to (35), q_n $(n=0,1,2)$ satisfies

$$(q_0)^a - 2(q_1)^a + (q_2)^a = 0, \tag{49}$$

for specified real number a. Therefore, the three unknown variables q_0, q_1 and q_2 are determined from equations (47), (48) and (49), in principle, and γ_1, γ_2 are given by

$$\gamma_1 = \gamma_0 + q_0\begin{pmatrix}\cos(\theta_1-\kappa)\\ \sin(\theta_1-\kappa)\end{pmatrix}, \quad \gamma_2 = \gamma_1 + q_1\begin{pmatrix}\cos(\theta_1-2\kappa)\\ \sin(\theta_1-2\kappa)\end{pmatrix}. \tag{50}$$

It is straightforward to generalize the above procedure to generate a dLAC with $N+2$ points, $\gamma_0 = {}^t(0,0), \gamma_1, \dots, \gamma_N, \gamma_{N+1} = {}^t(\ell,0)$, for given γ_0, γ_1 and γ_N, γ_{N+1} being on the respective edges of the specified triangle depicted in the second picture of Fig. 7. Then, q_n $(n=0,\dots,N)$ satisfy the following equations:

$$(q_{n-1})^a - 2(q_n)^a + (q_{n+1})^a = 0, \quad n=1,\dots,N-1, \tag{51}$$

$$q_0\cos\theta_1 + q_1\cos(\theta_1-\kappa) + \cdots + q_N\cos(\theta_1-N\kappa) = \ell, \tag{52}$$

$$q_0\sin\theta_1 + q_1\sin(\theta_1-\kappa) + \cdots + q_N\sin(\theta_1-N\kappa) = 0, \tag{53}$$

where $\kappa = \theta_2/N$. It is possible to determine q_n in principle, since we have $N+1$ equations for $N+1$ unknown variables q_n $(n=0,\dots,N)$. Then, we have

$$\gamma_n = \gamma_{n-1} + q_{n-1}\begin{pmatrix}\cos(\theta_1-n\kappa)\\ \sin(\theta_1-n\kappa)\end{pmatrix}, \quad n=1,\dots,N. \tag{54}$$

Now, equations (51)–(53) may be solved numerically as follows:

(1) We may write the general solution of (51) as

$$(q_n)^a = \frac{(N-n)(q_0)^a + n(q_N)^a}{N} \quad (n=0,\dots,N). \tag{55}$$

Also, we may temporarily put $(q_0)^a = \frac{\ell}{N+1}$.

(2) Substituting the above expressions into (53), we have a nonlinear equation in q_N. We then solve the equation by a suitable solver, e.g., the bisection method.

(3) Compute q_n $(n=1,\dots,N-1)$ by using (55).

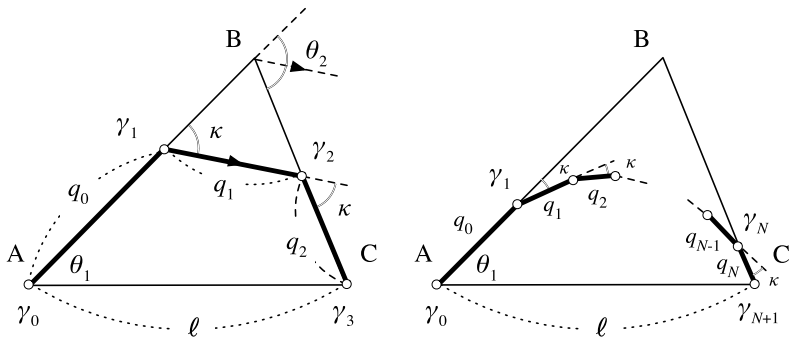

Fig. 7. Generation of discrete log-aesthetic curves by G^1 interpolation. Left: four points. Right: $N+2$ points.

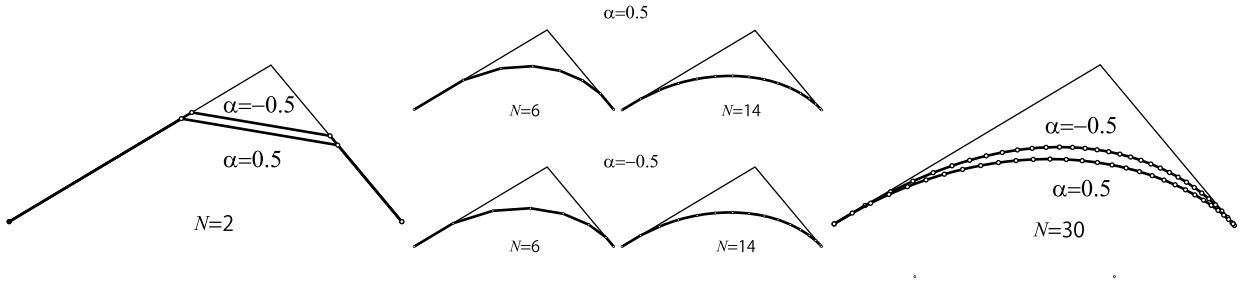

Fig. 8. Examples of discrete log-aesthetic curves with $N = 2, 6, 14, 30$ for $\alpha = \pm 0.5$.

(4) Compute the left-hand side of (52) and put it as L.
(5) Apply the scaling $T_n \to \frac{\ell}{L} T_n$ so that (52) is satisfied and regenerate γ_n.

In this method, we are able to reduce the nonlinear equations for q_n $(n = 0, \dots, N)$ to a single nonlinear equation for only one variable q_N, by using the linearity of (51) in $(q_n)^a$ and the scaling property of (52) and (53).

Fig. 8 illustrates the examples of dLACs generated by the above method. Despite the different α values, the shape of the curves in the top and bottom rows of the middle picture are similar. When $N = 2$ (total number of vertices is 4), the triangle cut by the vertices polyline of $\alpha = 0.5$ is a little bit larger than that of $\alpha = -0.5$ as shown in the superimposed figure on the left. The right figure illustrates the case of $N = 30$ for $\alpha = \pm 0.5$ and the area bounded by the control polyline with the curve for $\alpha = 0.5$ is larger than that with the one for $\alpha = -0.5$, that is consistent with the left and middle figures. Each curve reasonably approximates its continuous counterpart and the difference of those curves is reasonable when compared with the case of the smooth LAC as in Yoshida and Saito (2006). The discrete curvature of the curves (see Remark 3.1) is monotonically increasing from left to right and reproducing the smooth LAC's property very well. The computation time to generate dLACs on a Core i7 6700 3.4 GHz is from 10 to 20 msec according to $N = 50$ to 300 implemented in Matlab®. The computation time based on numerical discretization of the smooth LAC described in Yoshida and Saito (2006) takes about 80 msec in Matlab® and the discrete implementation is much faster since fine numerical integration to obtain the shape of the curves is not required and only coarse summation expressed in (54) to keep the boundary conditions are necessary.

The above advantage may be understood to be due to the geometric characterization of dLACs themselves as discrete curves. Namely, in similarity geometry, the turning angles of the discrete plane curves are constant κ, so that the shape is controlled by the segment length q_n. Since a discrete analogue of the curvature is given by $(2/q_n)\tan(\kappa/2)$, which is the reciprocal of the radius of the osculating circle touching the three consecutive edges (see Remark 3.1), if the curvature is large (resp. small) the segment length is small (resp. large). Therefore the distribution of the vertices is dense (resp. coarse) where the curvature is large (resp. small), which implies that the discrete plane curve under similarity geometry is regarded as a self-adaptive discretization, as illustrated in Fig. 9. Even a coarse discrete curve can generate sufficiently good shape. Especially, during the design stage, a designer tries to generate as various as possible curves as to pursue the desired shape. Coarse discrete curves are good enough and desirable because one can generate curves quickly and check their suitability.

5.2. Discrete log-aesthetic curves with an inflection

In this section, we propose a method generating a dLAC with an inflection, i.e., an S-shaped dLAC based on similarity geometry.

Unlike the case where there is no inflection discussed in Section 5.1, uniqueness of the solution is not guaranteed. As in the previous section, we assume that the discrete curve has $(N+2)$-vertices $\gamma_0 = {}^t(0,0), \gamma_1, \dots, \gamma_N, \gamma_{N+1} = {}^t(\ell, 0)$ $(\ell > 0)$.

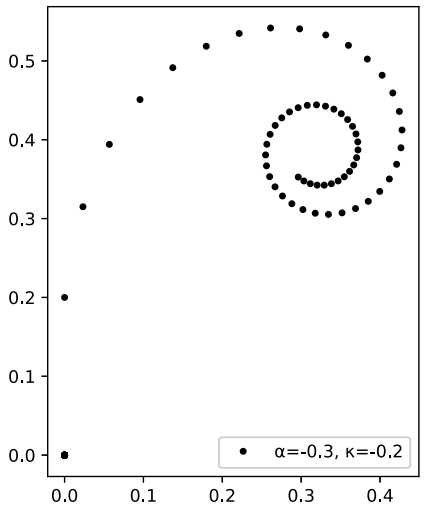

Fig. 9. Example of discrete log-aesthetic curves as a self-adaptive discretization of log-aesthetic curves. $\alpha = 0.3$, $\kappa = -0.2$, $\gamma_0 = (0, 0)$, $\gamma_1 = (0, 0.2)$.

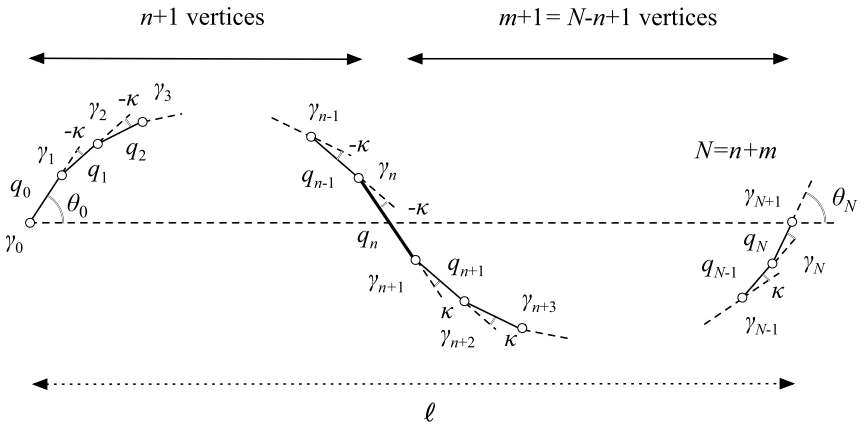

Fig. 10. A discrete log-aesthetic curve with an inflection.

Suppose that for given $n \in \{1, 2, \ldots, N-1\}$ the turning angles at the vertices $\gamma_1, \ldots, \gamma_n$ are a constant $-\kappa\,(<0)$, and those at $\gamma_{n+1}, \ldots, \gamma_N$ are $\kappa\,(>0)$. The edge $\gamma_n - \gamma_{n+1}$ corresponds to the "*inflection edge*" where the turning angles change the sign at the left and right vertices. We put $N - n = m$ so that there are $n+1$ vertices in the left of the inflection edge and $m+1$ vertices in the right (Fig. 10). The Euclidean curvature $\kappa(s)$ (s: arc length) of a smooth LAC with an inflection point is given by Miura et al. (2013)

$$\kappa(s) = \begin{cases} (c_0 s + c_1)^{-\frac{1}{\alpha}} & c_0 s + c_1 \geq 0, \\ -(-c_0 s - c_1)^{-\frac{1}{\alpha}} & \text{otherwise}, \end{cases} \tag{56}$$

where c_0, c_1 are parameters. We introduce the segment length q_k $(k = 0, 1, \ldots, N)$ as

$$q_k = \begin{cases} z(n-k+\delta)^{1/a}, & k = 0, \ldots, n-1, \\ z\delta^{1/a} & k = n, \\ z(-n+k+\delta)^{1/a}, & k = n+1, \ldots, N, \end{cases} \tag{57}$$

where $z, \delta > 0$ are parameters to be determined. The segment lengths have been chosen by the following consideration. We first specify the "inflection edge" length q_n. In view of (56), we then introduce the other segment lengths q_k in a symmetric manner with respect to q_n. Then q_k $(k = 0, \ldots, N)$ satisfies the following equations:

$$\sum_{i=0}^{n-1} q_i \cos(\theta_0 - i\kappa) + q_n \cos(\theta_0 - n\kappa) + \sum_{j=1}^{m} q_{n+j} \cos(\theta_0 - n\kappa + j\kappa) = \ell, \tag{58}$$

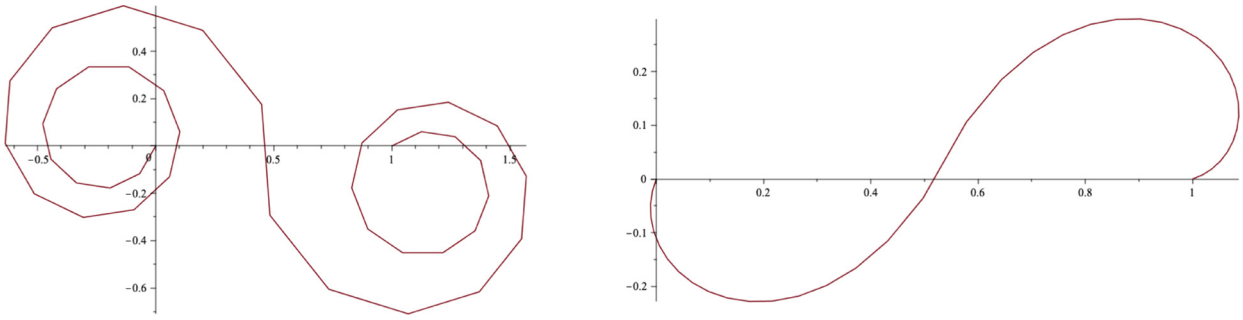

Fig. 11. Example of discrete log-aesthetic curves with an inflection to be excluded.

$$\sum_{i=0}^{n-1} q_i \sin(\theta_0 - i\kappa) + q_n \sin(\theta_0 - n\kappa) + \sum_{j=1}^{m} q_{n+j} \sin(\theta_0 - n\kappa + j\kappa) = 0, \tag{59}$$

$$\theta_0 - n\kappa + m\kappa = \theta_N. \tag{60}$$

From (60) we have

$$\kappa = \frac{\theta_N - \theta_0}{m - n}. \tag{61}$$

For a given number of vertices $N+2$, the slope $a = \alpha - 1$, the endpoints γ_0, γ_{N+1}, the angles θ_0, θ_N at γ_0, γ_{N+1}, respectively, and the position of the inflection n, one can compute the pair (δ, z) by solving (58) and (59) and the dLAC with an inflection can be generated accordingly. It should be remarked that in the discrete case, n must be prescribed and cannot be determined from the equations, so that the dLAC cannot be uniquely determined, while in the smooth case a LAC with an inflection point can be uniquely determined under a certain moderate condition (Miura et al., 2013).

However, if we prescribe the position of the inflection point n, sometimes there is no solution δ, or the triplet (n, δ, z) generates the discrete curve with undesirable shape in view of a design requirement as illustrated in Fig. 11. Therefore we impose the following assumptions in order to guarantee the existence of the solution and exclude the discrete curves described in Fig. 11,

$$\theta_0 - (n-l)\kappa \geq -\frac{\pi}{2}, \quad \text{for all} \quad l = 0, 1, 2, \ldots, \tag{62}$$

$$\theta_0 - n\kappa \leq 0. \tag{63}$$

Equations (62) and (63) are for excluding the dLACs in the left and the right of Fig. 11, respectively. Then we have the following restriction for the position of the inflection n, that is, an arbitrary choice of n is not allowable:

Lemma 5.1. *Assume that $\kappa > 0$. Then we have the following estimate:*

$$\begin{aligned} &\frac{\theta_0 + \frac{\pi}{2}}{\theta_0 + \theta_N + \pi} N \leq n \leq \frac{\theta_0}{\theta_0 + \theta_N} N, \quad (\theta_0 > \theta_N), \\ &\frac{\theta_0}{\theta_0 + \theta_N} N \leq n \leq \frac{\theta_0 + \frac{\pi}{2}}{\theta_0 + \theta_N + \pi} N, \quad (\theta_0 < \theta_N). \end{aligned} \tag{64}$$

Proof. We consider the first case. From the conditions (61), (62) and $N = n + m$, we have

$$\begin{aligned} 0 &\leq \theta_0 - (n-l)\kappa + \frac{\pi}{2} = \theta_0 - (n-l)\frac{\theta_N - \theta_0}{m-n} + \frac{\pi}{2} \\ &= \frac{1}{m-n}\left(-(\theta_0 + \theta_N + \pi)n + (\theta_N - \theta_0)l + \left(\theta_0 + \frac{\pi}{2}\right)N\right). \end{aligned}$$

Since the assumptions $\theta_N - \theta_0 < 0$ and $\kappa > 0$ give $m - n < 0$, we have

$$-(\theta_0 + \theta_N + \pi)n + (\theta_N - \theta_0)l + \left(\theta_0 + \frac{\pi}{2}\right)N \leq 0.$$

Therefore we conclude

$$n \geq \max_{l=0,1,\ldots,n} \frac{\left(\theta_0 + \frac{\pi}{2}\right)N + (\theta_N - \theta_0)l}{\theta_N + \theta_0 + \pi} = \frac{\theta_0 + \frac{\pi}{2}}{\theta_N + \theta_0 + \pi} N,$$

where we used the condition $l \geq 0$. The remaining part of the estimate can be shown in a similar manner. By the assumption (63), we have

$$0 \geq \theta_0 - n\kappa = \theta_0 - n\frac{\theta_N - \theta_0}{m-n} = \frac{m\theta_0 - n\theta_N}{m-n} = \frac{-n(\theta_0+\theta_N) + N\theta_0}{m-n}.$$

The condition $m - n < 0$ implies that the numerator of the last expression is non-negative, and therefore we have

$$n \leq \frac{\theta_0}{\theta_0+\theta_N} N,$$

which proves the first case. The second case is proved in a similar manner noting that $m - n > 0$. □

In summary, one can compute (δ, z) to generate a dLAC with an inflection from the given data $(N, a, \gamma_0, \gamma_{N+1}, \theta_0, \theta_N)$ for each n in the range in (64) as follows:

(1) Put $z = 1$ and solve (59) to obtain δ.
(2) Compute the left hand side of (58), and put it as L.
(3) Compute $|\gamma_{N+1} - \gamma_0| = \ell$ and put $z = \frac{\ell}{L}$.

This computation generates many dLACs and the choice may be left to the user, but a criteria may be given as follows. Consider the discrete fairing energy

$$\Phi^{\lambda,a}(\gamma) = \sum_{k=0}^{N-1} \left\{ (u_k)^a + \frac{1}{(u_k)^a} + \lambda \left(\frac{q_0 q_N}{q_k q_{k+1}} \right)^a \right\}, \tag{65}$$

whose Euler-Lagrange equation is given by

$$(u_k)^a - (u_{k-1})^a + \lambda \left(\frac{q_0 q_N}{q_{k-1} q_k} \right)^a = 0. \tag{66}$$

We compute the discrete fairing energy for a dLAC. Since $u_k = q_{k+1}/q_k$ with q_k in (57), λ can be determined from (66) as

$$\begin{aligned}\lambda &= -\Big((u_k)^a - (u_{k-1})^a \Big) \left(\frac{q_{k-1} q_k}{q_0 q_N} \right)^a = -\frac{(q_{k+1})^a (q_{k-1})^a - (q_k)^{2a}}{(q_{k-1})^a (q_k)^a} \left(\frac{q_{k-1} q_k}{q_0 q_N} \right)^a \\ &= -\frac{\big((q_k)^a + z^a\big)\big((q_k)^a - z^a\big) - (q_k)^{2a}}{(q_{k-1})^a (q_k)^a} \left(\frac{q_{k-1} q_k}{q_0 q_N} \right)^a = \left(\frac{z^2}{q_0 q_N} \right)^a.\end{aligned}$$

Then a direct computation gives the discrete fairing energy for the dLAC as

$$\Phi^{\lambda,a}(\gamma) = \sum_{k=0}^{N-1} \left\{ (u_k)^a + \frac{1}{(u_k)^a} + \left(\frac{z^2}{q_k q_{k+1}} \right)^a \right\} = 2N + 2\left(\frac{2}{\delta} - \frac{1}{n+\delta} - \frac{1}{-n+N+\delta} \right). \tag{67}$$

In view of the continuum limit to the LAC, we may choose the dLAC that attains the minimum of the discrete fairing energy (67). Practically, we may choose the dLAC corresponding to the maximum value of δ among those generated, since (67) is monotonic decreasing with respect to $\delta > 0$ for each n, and the change of the energy with respect to n is much smaller than that with respect to δ. Fig. 12 shows various dLAC examples with an inflection edge. We specified $N = 39$, so the total number of the vertices is 41. $\alpha = -2/3$ and the direction angle θ_s at the start (leftest) vertex is equal to $\pi/3$. We changed the direction angle θ_e at the end (rightest) vertex to be $\pi/12$, $\pi/6$ and $\pi/4$. The edge in red is an inflection edge in each curve. The sign of the discrete turning angle κ of the curve segment in green is negative and that in blue is positive. For $\theta_e = \pi/12$, there are 6 solutions for (δ, z) although for $\theta_e = \pi/6$ and θ_e, 3 and 2 solutions exist, respectively. For each curve, we described its corresponding (n, δ) values. As n increases, δ decreases. The discrete fairing energy is the lowest for the leftest curve in each group, in which its inflection edge is the shortest.

We now consider the construction of the continuous representation of dLACs, which is indispensable especially for manufacturing to guarantee the precision of the products to be made. Through this process, the variety of dLACs generated under the same condition in Fig. 12 serves as a flexibility of the shape generation so that the designer can select the desirable shape.

For an S-shaped dLAC consisting of three parts, we have approximated the first and third parts by B-spline curves with the least square method and for the inflection edge, we have generated a Bézier curve with G^2 continuity. Fig. 13 shows a B-spline curve approximation of the dLAC example with $(n, \delta) = (28, 0.054822)$ whose direction angle at the end vertex is $\pi/12$ in Fig. 12. Its left figure shows two quartic B-spline curves approximating the first and third part of the dLAC and a quintic Bézier curve approximating the inflection edge. Its right figure shows discrete curvature of the dLAC by small circles

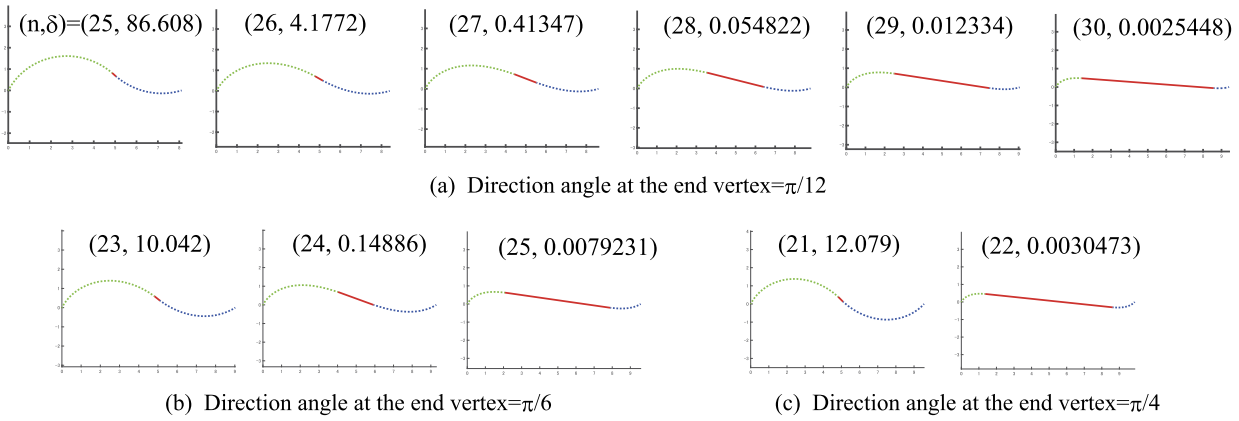

Fig. 12. Examples of discrete log-aesthetic curves with $\alpha = -2/3$, $N = 39$ and their direction angles θ_s at the start vertices is $\pi/3$.

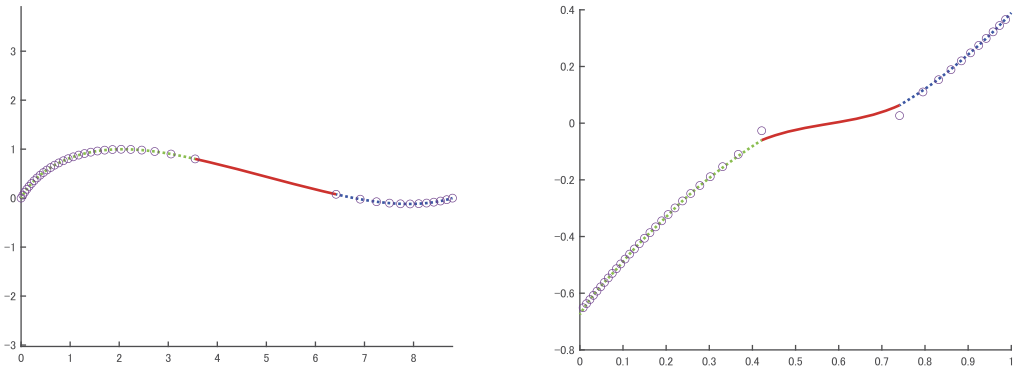

Fig. 13. B-spline curve approximation of the examples of discrete log-aesthetic curves $(n, \delta) = (28, 0.054822)$ whose direction angle at the end vertex is $\pi/12$ in Fig. 12. Left: approximation curves, right: curvature distribution.

and continuous curvature of the B-spline and Bézier curves by continuous lines. Both of the discrete points and curvatures are well approximated by the continuous ones and G^2 continuity is guaranteed as shown in the figures. The reason why the approximation is good is that the discrete points of a dLAC do not have noises although measured points are inevitably with noise. In this way, the dLACs can be directly used for manufacturing, providing a flexible method of high-quality shape generation.

6. Conclusion and future works

In this paper, we have presented the new framework of the LAC and the qAC by exploiting the similarity geometry, where they are characterized as invariant curves with respect to the integrable evolution. The dLAC and the dqAC have been proposed as the integrable discretizations of the LAC and the qAC, respectively, based on this framework. Also, the characterization by the variational principles for those curves has been presented. We have implemented the methods to generate both C-shaped and S-shaped dLACs, and demonstrated that they serve as a flexible method of high-quality shape generation through their continuous representations.

The dLAC may be particularly useful in the reverse engineering, where the shape is obtained as the discrete points data by the measurement. In this context, the fairing of a given discrete curve by the dLAC plays a crucial role in the design using the LAC.

We have presented a sound mathematical basis for the LAC and the qAC. Based on this, we aim to formulate natural generalizations of the LAC to space curves and surfaces, which are expected to be useful for generating “aesthetic” shapes in industrial design. Those issues will be reported in the future publications.

CRediT authorship contribution statement

Jun-ichi Inoguchi: Conceptualization, Writing-Original draft preparation. **Yoshiki Jikumaru:** Writing-Reviewing and Editing, Visualization. **Kenji Kajiwara:** Supervision, Conceptualization, Writing-Original draft preparation. **Kenjiro T. Miura:** Software, Visualization, Writing-Original draft preparation. **Wolfgang K. Schief:** Conceptualization, Writing-Original draft preparation.

Declaration of competing interest

The authors declare that they have no known competing financial interests or personal relationships that could have appeared to influence the work reported in this paper.

Data availability

No data was used for the research described in the article.

Acknowledgement

This work was supported by JST CREST Grant Number JPMJCR1911. It was also supported by JSPS KAKENHI Grant Numbers JP19K03461, JP19H02048, JP25289021, JP16H03941, JP16K13763, JP15K04834, JP26630038, JP23K03081, JST RISTEX Service Science, Solutions and Foundation Integrated Research Program, and ImPACT Program of the Council for Science, Technology and Innovation. The authors acknowledge the support by 2016 and 2018 IMI Joint Use Program Short-term Joint Research "Differential Geometry and Discrete Differential Geometry for Industrial Design" (Grant Numbers 20160009, 20180008). The authors would like to express their sincere gratitude to Prof. Miyuki Koiso, Prof. Hiroyuki Ochiai, Prof. Nozomu Matsuura, Prof. Sampei Hirose and Prof. Takashi Maekawa for invaluable comments and fruitful discussions. The authors also thank the reviewers who carefully read the manuscript and provided many valuable comments.

References

Albayari, D.J., Gobithaasan, R.U., Miura, K.T., 2017. The approximation of generalized Log-aesthetic curves using Quintic Bezier curves. Inst. Phys. Conf. Ser. 890, 0120.

Chou, K.-S., Qu, C.-Z., 2002. Integrable equations arising from motions of plane curves. Phys. D 162, 9–33. https://doi.org/10.1016/S0167-2789(01)00364-5.

Gobithaasan, R.U., Karpagavalli, R., Miura, K.T., 2014a. G^2 continuous generalized log-aesthetic curves. Comput-Aided Des. Appl. 12 (2), 192–197. https://doi.org/10.1080/16864360.2014.962431.

Gobithaasan, R.U., Miura, K.T., 2011. Aesthetic spiral for design. Sains Malays. 40 (11), 1301–1305.

Gobithaasan, R.U., Miura, K.T., Yee, L.P., Wahab, A.F., 2014b. Aesthetic curve design with linear gradients of logarithmic curvature/torsion graphs. Mod. Appl. Sci. 8 (3), 24–30. https://doi.org/10.5539/mas.v8n3p24.

Gobithaasan, R.U., Teh, Y.M., Piah, A.R.M., Miura, K.T., 2014c. Generation of Log-aesthetic curves using adaptive Runge-Kutta methods. Appl. Math. Comput. 246 (1), 257–262. https://doi.org/10.1016/j.amc.2014.08.032.

Gobithaasan, R.U., Wei, Y.S., Miura, K.T., 2014d. Log-aesthetic curves for shape completion problem. J. Appl. Math. 2014 (3), 1–10. https://doi.org/10.1155/2014/960302.

Harada, T., Yoshimoto, F., Moriyama, M., 1999. An aesthetic curve in the field of industrial design. In: Proceedings 1999 IEEE Symposium on Visual Languages, pp. 38–47.

Hirota, R., 1979. Nonlinear partial difference equations. V: Nonlinear equations reducible to linear ones. J. Phys. Soc. Jpn. 49, 312–319. https://doi.org/10.1143/JPSJ.46.312.

Hoffmann, T., 2009. Discrete Differential Geometry of Curves and Surfaces. MI Lecture Notes, vol. 18. Kyushu University, Fukuoka.

Inoguchi, J., 2016. Attractive plane curves in differential geometry. In: Dobashi, Y., Ochiai, H. (Eds.), Mathematical Progress in Expressive Image Synthesis III. In: Mathematics for Industry, vol. 24. Springer, Singapore, pp. 121–135.

Inoguchi, J., Kajiwara, K., Miura, K.T., Sato, M., Schief, W.K., Shimizu, Y., 2018. Log-aesthetic curves as similarity geometric analogue of Euler's elasticae. Comput. Aided Geom. Des. 61, 1–5. https://doi.org/10.1016/j.cagd.2018.02.002.

Inoguchi, J., Ziatdinov, R., Miura, K.T., 2019. Generalization of log-aesthetic curves via similarity geometry. Jpn. J. Ind. Appl. Math. 36, 239–259. https://doi.org/10.1007/s13160-018-0335-7.

Kajiwara, K., Kuroda, T., Matsuura, N., 2016. Isogonal deformation of discrete plane curves and discrete Burgers hierarchy. Pac. J. Math. Ind. 8 (3). https://doi.org/10.1186/s40736-016-0022-z.

Kobayashi, S., Kimura, F., 2010. Method for curve and surface generation with smooth curvature change by reconstructing connection points based on discrete geometry models. J. Jpn. Soc. Precis. Eng. 76 (9), 1059–1063 (in Japanese).

Lu, L., Xiang, X., 2016. Quintic polynomial approximation of log-aesthetic curves by curvature deviation. J. Comput. Appl. Math. 296, 389–396. https://doi.org/10.1016/j.cam.2015.10.002.

Miura, K.T., 2006. A general equation of aesthetic curves and its self-affinity. Comput-Aided Des. Appl. 3 (1–4), 457–464. https://doi.org/10.1080/16864360.2006.10738484.

Miura, K.T., Shibuya, D., Gobithaasan, R.U., Usuki, S., 2013. Designing log-aesthetic splines with G^2 continuity. Comput-Aided Des. Appl. 10 (6), 1021–1032.

Miura, K.T., Gobithaasan, R.U., 2014. Aesthetic curves and surfaces in computer aided geometric design. Int. J. Autom. Technol. 8 (3), 304–316. https://doi.org/10.20965/ijat.2014.p0304.

Miura, K.T., Gobithaasan, R.U., 2016. Aesthetic design with log-aesthetic curves and surfaces. In: Dobashi, Y., Ochiai, H. (Eds.), Mathematical Progress in Expressive Image Synthesis III. In: Mathematics for Industry, vol. 24. Springer, Singapore, pp. 107–119.

Miura, K.T., Gobithaasan, R.U., Suzuki, S., Usuki, S., 2015. Reformulation of generalized log-aesthetic curves with Bernoulli equations. Comput-Aided Des. Appl. 13 (2), 265–269. https://doi.org/10.1080/16864360.2015.1084200.

Miura, K.T., Suzuki, S., Gobithaasan, R.U., Salvi, P., Usuki, S., 2017. Log-aesthetic flow governed by heat conduction equations. Comput-Aided Des. Appl. 14 (2), 227–233. https://doi.org/10.1080/16864360.2016.1223436.

Miura, K.T., Suzuki, S., Gobithaasan, R.U., Usuki, S., Inoguchi, J., Sato, M., Kajiwara, K., Shimizu, Y., 2018. Fairness metric of plane curves defined with similarity geometry invariants. Comput-Aided Des. Appl. 15 (2), 256–263. https://doi.org/10.1080/16864360.2017.1375677.

Nishinari, K., Takahashi, D., 1998. Analytical properties of ultradiscrete Burgers equation and rule-184 cellular automaton. J. Phys. A, Math. Theor. 31, 5439–5450. https://doi.org/10.1088/0305-4470/31/24/006.

Sato, M., Shimizu, Y., 2015. Log-aesthetic curves and Riccati equations from the viewpoint of similarity geometry. JSIAM Lett. 7, 21–24. https://doi.org/10.14495/jsiaml.7.21.

Sato, M., Shimizu, Y., 2016. Generalization of log-aesthetic curves by Hamiltonian formalism. JSIAM Lett. 8, 49–52. https://doi.org/10.14495/jsiaml.8.49.

Suzuki, T., 2017. Application of Log-aesthetic curves to the roof design of a wooden house. In: Archi-Cultural Interactions Through the Silkroad, 4th International Conference. Mukogawa Women's University, Nishinomiya, Japan, July 16-18, 2016, Selected Papers, pp. 121–126.

Suzuki, S., Gobithaasan, R.U., Salvi, P., Usuki, S., Miura, K.T., 2018a. Minimum variation log-aesthetic surfaces and their applications for smoothing free-form shapes. J. Comput. Des. Eng. 5 (2), 243–248. https://doi.org/10.1016/j.jcde.2017.08.003.

Suzuki, S., Gobithaasan, R.U., Usuki, S., Miura, K.T., 2018b. A new formulation of the minimum variation log-aesthetic surface for scale-invariance and parameterization-independence. Comput-Aided Des. Appl. 15 (5), 661–666. https://doi.org/10.1080/16864360.2018.1441232.

Wo, M.S., Gobithaasan, R.U., Miura, K.T., 2014. Log-aesthetic magnetic curves and their application for CAD systems. Math. Probl. Eng. 2014, 504610. https://doi.org/10.1155/2014/504610.

Wo, M.S., Gobithaasan, R.U., Miura, K.T., Abbas, M., 2015. A note on G^2 log-aesthetic curves. AIP Conf. Proc. 1691, 040017. https://doi.org/10.1063/1.4937067.

Yoshida, N., Saito, Y., 2006. Interactive aesthetic curve segments. Vis. Comput. 22, 896–905. https://doi.org/10.1007/s00371-006-0076-5.

Ziatdinov, R., Yoshida, N., Kim, T., 2012. Analytic parametric equations of log-aesthetic curves in terms of incomplete gamma functions. Comput. Aided Geom. Des. 29 (2), 129–140. https://doi.org/10.1016/j.cagd.2011.11.003.